Kinetics and Mechanism of Carbamate Formation from CO_2(aq), Carbonate Species, and Monoethanolamine in Aqueous Solution

Nichola McCann,[†] Duong Phan,[†] Xiaoguang Wang,[†] William Conway,[†] Robert Burns,[†] Moetaz Attalla,[‡] Graeme Puxty,[‡] and Marcel Maeder*,[†]

Department of Chemistry, The University of Newcastle, Newcastle NSW 2308, Australia, and CSIRO Division of Energy Technology, P.O. Box 330, Newcastle NSW 2300, Australia

Received: July 14, 2008; Revised Manuscript Received: February 11, 2009

Removal of carbon dioxide from fossil-based power generation is a potentially useful technique for the reduction of greenhouse gas emissions. Reversible interaction with aqueous amine solutions is most promising. In this process, the formation of carbamates is an important reaction of carbon dioxide. In this contribution, a detailed molecular reaction mechanism for the carbamate formation between MEA (monoethanolamine) and dissolved CO_2 as well as carbonate species in aqueous solution is presented. There are three parallel, reversible reactions of the free amine with CO_2, carbonic acid, and the bicarbonate ion; the relative importance of the three paths is strongly pH dependent. Kinetic and equilibrium measurements are based on ^{1}H NMR and stopped-flow measurements with rate constants, equilibrium constants, and protonation constants being reported.

Introduction

Carbon dioxide is the major product of the combustion of organic matter, it is extremely stable, and thus is not very reactive. One major source of CO_2 in the atmosphere is energy production based on the combustion of fossil fuel. With the prospect of runaway global warming due to increasing CO_2 concentration in the atmosphere, research directed at options for reducing CO_2 output is crucial. An important technology for greenhouse gas reduction is the capture of CO_2 from the flue gases of fossil fuel-fired power stations, a process known as postcombustion capture or PCC.[1] The most widely applied technology for carbon capture is reversible absorption of CO_2 by aqueous amine solutions. This technology is well developed, e.g., for CO_2 removal from natural gas (gas sweetening) and in ammonia production. The investigation of the fundamental chemical processes pertinent to reversible amine-based carbon capture is highly relevant.

CO_2 reacts with water to form carbonic acid, $CO_2 + H_2O \rightleftarrows H_2CO_3$ and carbonic acid is involved in two protonation equilibria. The mechanism and its rate and equilibrium constants were published some 40 years ago.[2] The reaction includes two reversible pathways: the reversible interaction of CO_2 with water to form carbonic acid and with hydroxide to form bicarbonate. This research has been confirmed by theoretical studies in the gas phase.[3] In aqueous amine solutions additional reactions occur. One is the essentially instantaneous Brønstedt acid−base interaction between the carbonic acid and the amine which is quantitatively defined by the protonation constants for the carbonate system and the amine. Under prevailing conditions (pH) this is a 1:1 interaction. (Note, throughout this contribution, we use $\leftrightarrow$ arrows for instantaneous protonation equilibria and $\rightleftarrows$ for kinetically observable reactions and equilibria.)

$$\begin{aligned} &H_2CO_3 \leftrightarrow HCO_3^- + H^+ \\ &RNH_2 + H^+ \leftrightarrow RNH_3^+ \end{aligned} \quad (1)$$

The other important reaction is the formation of carbamic acid which at relevant pH is deprotonated to the carbamate, resulting in a 1:2 (CO_2:amine) stoichiometry. There are at least two different reaction paths: the interaction of the amine with carbonic acid and with dissolved CO_2

$$\begin{aligned} &2RNH_2 + H_2CO_3 \rightleftarrows RNHCO_2^- + RNH_3^+ + H_2O \quad \text{(a)} \\ &2RNH_2 + CO_2 \rightleftarrows RNHCO_2^- + RNH_3^+ \quad \text{(b)} \end{aligned} \quad (2)$$

The molecular efficiency or the ratio of the CO_2:amine interaction is crucially important. The higher the ratio the smaller the size and footprint of a capture plant and also the energy requirement per unit of CO_2 captured, as the energy requirement for the cyclic heating and cooling is strongly dependent on the total volume of absorber solution. For this reason the thorough investigation of carbamate formation is of utmost importance. In this contribution we report the detailed reaction mechanism of carbamate formation in aqueous solution for the example of monoethanolamine, MEA, including all relevant rate and equilibrium constants. MEA is one of the industrially most relevant amines for carbon capture.

To our knowledge there is no detailed mechanistic kinetic study of any amine that includes all the paths toward the formation of carbamates. First investigations were undertaken midlast century, resulting in selected empirical rate and equilibrium constants of a series of carbmates of ammonia, as well as propyl and butyl amines.[4−6] These were not based on a mechanistically complete model, e.g., they did not include all protonation equilibria. Reliable equilibrium constants for the interaction of CO_2 with ammonia and the protonation constant of the carbamate were published much later.[7] This early research was based on quenching the reaction by raising the pH and

* To whom correspondence should be addressed.
[†] The University of Newcastle.
[‡] CSIRO Energy Technology.

10.1021/jp810564z CCC: $40.75
Published on Web 04/01/2009

subsequent quantitative precipitation of the carbonates as $BaCO_3$. $BaCO_3$ precipitation of radiolabeled $^{14}CO_2$ is a similar technique.[8]

There is a considerable number of publications on carbamate formation in the chemical engineering literature. However, the research is directed toward the development of empirical functions and/or empirical mechanisms that achieve the modeling of the reaction under particular conditions; usually it is the interaction of CO_2 from the gas phase with aqueous amine solutions. These applied investigations do not primarily attempt the development of a molecular reaction mechanism that describes all reactions in solution, after the absorption of CO_2 from the gas phase. There are three published empirical reaction mechanisms that adequately model the measured gas absorption data. The most prominent mechanism involves the formation of a zwitterionic form of the carbamate followed by a slow proton exchange reaction with a base. This mechanism was originally proposed by Caplow[8] and has been used in many instances since then[9−11]

$$\begin{aligned} CO_2 + RNH_2 &\rightleftarrows RNH_2^+CO_2^- \\ RNH_2^+CO_2^- + B &\rightleftarrows RNHCO_2^- + BH^+ \end{aligned} \qquad (3)$$

Amides are very weak bases, and they are not known to protonate in aqueous solution, while the log of the protonation constant of carbamic acid with ammonia has been reported as 6.76,[7] and our result for the carbamate of MEA is 7.49(5) (see below). Thus, the concentration of the zwitterion of eq 3 must be insignificant compared with the tautomeric, neutral form of the carbamic acid. While this structural question is not of mechanistic importance, the proton exchange reaction as represented in the second step is diffusion controlled and essentially instantaneous, and thus the kinetics of this process cannot be observed.

Another suggested mechanism includes a formally termolecular reaction between CO_2, the amine, and a base[12]

$$B + RNH_2 + CO_2 \rightleftarrows RNHCO_2^- + BH^+ \qquad (4)$$

To our knowledge there are no known proper termolecular reactions. As before, they can be used to empirically describe observations; however, on a molecular basis they are always combinations of sequential lower order reactions. Theoretical computational studies of reaction paths often include additional water molecules;[13] however, this does not translate into high-order kinetics in aqueous solution.

Reactions of variable reaction order have also been used to describe measured data (see ref 14 and references therein). As with the mechanisms previously, variable reaction order can only be of an empirical nature, as there are clearly no fractions of molecules that undergo reactions.

A realistic mechanism is based on the direct reaction of the amine with dissolved CO_2, followed by the deprotonation of the carbamic acid in a normal protonation equilibrium.[15]

$$\begin{aligned} CO_2 + RNH_2 &\rightleftarrows RNHCO_2H \\ RNHCO_2H &\rightleftarrows RNHCO_2^- + H^+ \end{aligned} \qquad (5)$$

This mechanism is mechanistically feasible. It adequately describes the kinetics of the interaction of gaseous CO_2 with aqueous amine solutions in wetted-wall experiments. We will demonstrate in the experimental section that in basic aqueous solution with carbonate species as major components, mechanism 5 is not sufficient to explain the kinetics of formation of carbamate, and the reactions of the amines with carbonic acid and bicarbonate have to be included in the reaction mechanism.

Several authors base their investigations on the quantitative determination of CO_2 partial pressure in the gas phase above the reaction solution[10,15,16] in wetted-wall experiments. Such two-phase experiments suffer from relatively slow response times, and information on carbamate formation is very indirect and thus error prone.

A series of stopped-flow investigations, using conductometry[11] and pH determination via color changes due to a coupled indicator,[17−19] have been published. Both methods are fast. Proposed mechanisms describe the measured data adequately, but they are also based on empirical mechanisms. Ab initio studies have also been undertaken but without giving definite answers about the mechanism.[20,21]

A few NMR studies have been published. Quantitative ^{13}C NMR spectroscopy delivers direct information on the concentration of all carbon-containing species; however, ^{13}C NMR suffers from slow relaxation processes, and thus the acquisition of quantitative information via peak integrals is necessarily extremely slow. As a consequence, measuring times with accurate integration are too slow for the rates observed in our reactions. Publications of this type include studies on solubility of CO_2,[22] and quantitative speciation.[23,24] ^1H NMR has also been used for speciation purposes in amine CO_2 interactions.[25] Two very recent publications report the equilibria for several amine/CO_2 interactions using combined ^1H and ^{13}C NMR data.[24,26] All these studies concentrate on the thermodynamic equilibria and do not cover the kinetics. Another promising technique is IR spectroscopy;[27] it is relatively fast but to our knowledge no quantitative study on carbamate formation has been published.

In this study we use ^1H NMR spectroscopy and stopped-flow UV−vis spectroscopy to quantitatively investigate carbamate formation in aqueous MEA solutions. The measurements include kinetic as well as equilibrium experiments.

Experimental Section

Monoethanolamine (MEA) was obtained from Sigma-Aldrich, $KHCO_3$ from Sigma-Aldrich, and HCl from Ajax Finechem. MEA was distilled prior to use and the pure compound stored under N_2. All solutions were freshly made prior to each experiment. HCl concentrations were determined by titration with standardized NaOH on an automated titration apparatus. ^1H NMR spectra were recorded on a Bruker Avance DPX-300 at a frequency of 300.13 MHz at 30.0 °C. All samples were measured in H_2O in a 5 mm tube containing an insert with TSP (3-(trimethylsilyl)propionic acid-d_4, sodium salt) in D_2O as a reference. All measurements were conducted in duplicate. Stopped-flow data were acquired at 30.0 °C on an Applied Photophysics DX-17 spectrophotometer equipped with a J&M Tidas MCS 500-3 diode-array detector.

NMR Analyses. MEA and its carbamate are the only ^1H NMR active species other than H_2O. Both molecules feature two neighboring methylene groups that give rise to two multiplets (both indicated in bold characters in the eqs 6 and 7). In the pH region investigated in this work, both species are involved in pH-dependent protonation equilibria at the primary amine for MEA and the carboxylate group of the carbamate.

$$HO\mathbf{CH_2CH_2}NH_2 + H^+ \leftrightarrow HO\mathbf{CH_2CH_2}NH_3^+ \qquad (6)$$

$$HOCH_2CH_2NHCO_2^- + H^+ \leftrightarrow HOCH_2CH_2NHCOOH \quad (7)$$

As a consequence, the chemical shifts of the two multiplets are pH-dependent, and the peak integrals represent the sum over the concentrations of the protonated and deprotonated forms. If possible, both methylene integrals were evaluated for the two species; however, at some pH values the peaks partially overlap. No attempt was made to deconvolute these integrals into the contributions of the two components; in these instances only one integral was used for quantification. The availability of two integrals, which should be identical, allows an estimate of the uncertainty of the determination. It is about 2−3%. This is also reflected in the spread of measurement shown with markers in Figure 3.

The sum of the concentrations of protonated and deprotonated MEA and the sum of the concentrations of carbamate and carbamic acid are determined from NMR data via their relative integrals. They were utilized in the subsequent nonlinear least-squares fits.

All NMR tubes were filled close to the top and loosely stoppered. Only measurements with $[CO_2(aq)] < 30$ mM were used for analysis. Under these conditions the partial pressure of CO_2 in the gas phase is below atmospheric pressure and losses of $CO_2(aq)$ into the gas phase are minimal.

Kinetics. Aqueous solutions of MEA/HCl and solutions of $KHCO_3$ were mixed manually and transferred to NMR tubes. The initial spectrum was measured typically 2−3 min after mixing, and subsequent spectra were measured automatically at a frequency and time scale appropriate for the rate of the reaction. Prior to, and during mixing and measurement, solutions were thermostatted at 30 °C. Three types of kinetic measurements were acquired; they differ by the initial concentration of the reactants. For type a, the initial concentrations were $[MEA]_{tot} = 2.28$ M, $[CO_3^{2-}]_{tot} = 1.64$ M, and $[H^+]_{tot} = 1.64$ M; for type b, the concentrations were $[MEA]_{tot} = 4.19$ M, $[CO_3^{2-}]_{tot} = 0.50$ M and $[H^+]_{tot} = 4.23$ M; for type c, the initial concentrations were $[MEA]_{tot} = 3.01$ M, $[CO_3^{2-}]_{tot} = 1.20$ M, and $[H^+]_{tot} = 2.83$ M. Note, the notation $[H^+]_{tot}$ represents the total concentration of available protons (excluding water), $[H^+]_{tot} = [HCl] + [HCO_3^-] + 2[H_2CO_3] + [AH] + [ACO_2H]$; the same holds for the total concentrations of amine $[A]_{tot}$ and carbonate species $[CO_3^{2-}]_{tot}$. These concentrations were chosen to cover all the amine and carbonate concentration and pH ranges required to deliver information about the different mechanistic steps. Each measurement was repeated, and all six data sets were fitted globally, i.e., all parameters for the different models that were tested were fitted to all measurements together. The concentrations as determined from resolved peak integrals were used in the fitting. All concentrations for kinetic and equilibrium NMR measurements are included in the Supporting Information.

Equilibria. Two types of titrations were performed. In the first, type a, aliquots of $KHCO_3$ were added to solutions of MEA/HCl; the concentration ranges were $[MEA]_{tot} = 5.0-3.1$ M, $[CO_3^{2-}]_{tot} = 0-1.1$ M, and $[H^+]_{tot} = 4.5-4.0$ M. In the second, type b, aqueous solutions of MEA/$KHCO_3$ were prepared and aliquots of HCl added; the concentration ranges were $[MEA]_{tot} = 4.0-2.5$ M, $[CO_3^{2-}]_{tot} = 3.0-1.9$ M, and $[H^+]_{tot} = 3.0-3.7$ M. In both cases, all mixtures were maintained at 30 °C for approximately 5 h prior to measurement to ensure complete equilibration. Again, concentrations were chosen in order for the experiments to deliver information about the relevant equilibria.

Figure 1 displays an equilibrium measurement of type b, addition of HCl to a solution of MEA/HCO_3^-. At the beginning of the titration, the pH is approximately 10, the amine is predominantly deprotonated and its NMR peaks are at 2.6 ppm for the NCH_2 and at 3.4 ppm for the OCH_2 groups. Upon addition of hydrochloric acid, the amine is gradually protonated and both peaks shift downfield to around 3 ppm and 3.6 ppm; the *N*-methylene group is more strongly affected and shifts by a larger extent. The relative concentration of amine (protonated + deprotonated) increases from 30% to 100% during this process. The carbamate concentration (protonated + deprotonated) changes in a balancing manner from 70% to 0%. At high pH the *N*-methylene group of the carbamate appears at around 3 ppm, and the *O*-methylene group at 3.4 ppm. Its protonation occurs at lower pH, and the shifts are smaller and not discernible in this graph. At high pH the NCH_2 peaks are used for the quantitative analysis, and at low pH the OCH_2 peaks. Figure 3B represents the concentration profiles graphically, and the actual concentrations are listed in the Supporting Information. Note the carbamate peak close to 3 ppm is a pseudoquartet due to the coupling with the amide proton; this has been confirmed by COSY measurements in H_2O and also exchange studies in D_2O where the amide proton exchanges and the quartet transforms into a triplet. In the subsequent spectrum in Figure 1, this peak is broad due to intermediate time scale exchange processes in the slightly more acidic solution. In the next spectrum the peak appears as a triplet, indicating fast exchange in the more acidified solution.

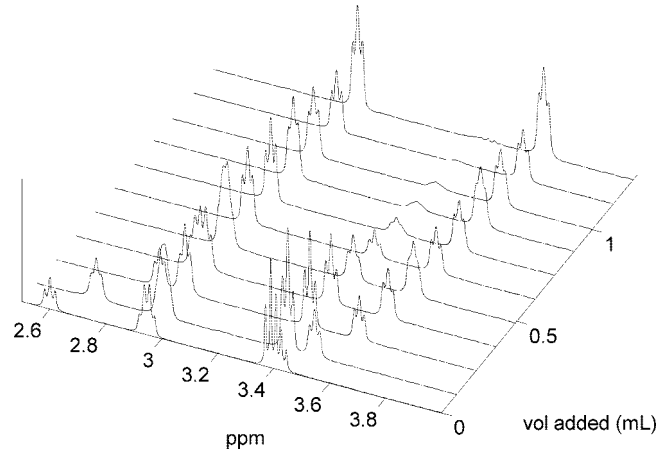

Figure 1. Titration of a MEA/HCO_3^- solution with HCl (see also Figure 3(B) for the concentration profiles for this reaction, last four spectra removed). See text for interpretation of the peaks.

Stopped-Flow Measurements. The fast reaction between dissolved CO_2 and MEA was investigated using stopped-flow technology, observing pH changes via coupling to thymol blue indicator.[28] There is a wide range of published rate constants for this reaction.[29] Although two recent values agree very closely,[30,31] we decided to reinvestigate this reaction, also in view of the fact that no rates for the reverse reaction have been published.

The reaction was initiated by mixing aqueous solutions of MEA and thymol blue with CO_2/N_2 saturated water to result in initial concentrations of $[MEA]_0 = 2.0$, 4.0, 6.0 mM, $[CO_2]_0 = 3.8$, 6.4, and 8.5 mM, and [indicator] = 0.1 mM. Absorption spectra from 400−700 nm were acquired in 2.5 ms intervals for total measurement times of 0.1 to 0.5 s, depending on the reaction. Each of the nine measurements was repeated five times. $[CO_2]_0$ was calculated from relative gas flow rates of N_2 and CO_2, assuming ideal behavior, and the published saturation concentration.[32] Absorption changes were due to the protonation of thymol blue as a result of the release of a proton from the

carbamic acid that formed. The protonation of MEA was taken into account. All solutions were thermostatted at 30 °C before and during the measurements.

Data Analysis. Modeling of the concentrations of the reacting species as a function of the process studied is the core of any data fitting algorithm. For the equilibrium studies, the concentrations of protonated and deprotonated MEA and its carbamate were modeled based on the known total concentrations of all components using standard Newton−Raphson techniques.[33] The modeling of the kinetic data was more complex. Standard numerical integration of the pertinent systems of differential equations was not possible because the pH varied considerably during the reactions. Buffering of the solutions was clearly out of question because of high concentrations of the reactants and unavoidable interactions of the buffer components with either the amine or the CO_2/H_2O system. Recently developed algorithms that take into account process-induced pH changes and subsequent adjustment of the protonation equilibria have been employed.[34]

For both equilibrium and kinetic studies, activity coefficient corrections were applied to all charged species. Estimates for the activity coefficients were calculated by the extended Debye−Hückel equation, eq 8,[35] which has been used for the simulation of enthalpy and capacity of CO_2 absorption by aqueous amine solutions.[36]

$$\log \gamma_i = \frac{-Az_i^2\sqrt{\mu}}{1 + Br_i\sqrt{\mu}} \tag{8}$$

The activity coefficient γ_i is a function of the ionic strength μ, the charge z_i of the ith component and of the parameters A and B that are defined by the dielectric constant of the solvent and the temperature. In water at 30 °C, $A = 0.51$, $B = 0.33$. The radii r_i are not known for several of the ionic species; the values were estimated based on published values for similar compounds.[37,38]

It has to be mentioned that the ionic strength correction is not expected to be perfect, particularly at the high concentrations required for the investigation of relevant solution concentrations. As a result, ionic strength changes during the reactions are significant. While not perfect such corrections are useful and certainly superior to the alternative of ignoring them altogether.[39]

Nonlinear least-squares fitting of the relevant parameters, rate or equilibrium constants, was based on standard Newton−Gauss−Levenberg/Marquardt algorithms which also deliver error estimates for the fitted parameters.[33,40] All kinetic measurements, including NMR and stopped-flow data, were analyzed together in one global analysis.

Results

Data fitting, based on a molecular reaction mechanism, requires a list of all interactions between any of the species that occur at any moment during the process investigated. In order to develop such a reaction model, first, a complete list of all species that exist in the solutions needs to be established, and second, all significant reactions between the different species need to be identified. These reactions include instantaneous equilibria, quantitatively defined by equilibrium constants, and kinetically observable reactions, defined by rate constants. The subsequent goal of the data fitting is to determine the equilibrium and rate constants of these reactions.

There are three groups of species relevant for the interaction of primary monoamines with CO_2. The first group includes all species of the carbon dioxide/carbonate family, i.e., dissolved CO_2, CO_2(aq), and its reaction products with water which include carbonic acid as well as the bicarbonate and carbonate ions. The chemistry of CO_2 in aqueous solution is well-known.[2,41] The kinetically observable, relatively slow reactions include the reversible interactions of CO_2 with either H_2O or OH^- to form carbonic acid and bicarbonate, respectively. These reactions are coupled to the protonation equilibria of carbonic acid which are diffusion controlled and thus too fast to be observable with traditional methods. Table 1 lists all these reactions and their rate and/or equilibrium constants. The protonation constants of many amines are known;[42] the value for MEA is listed in Table 1.

The second group of potentially reactive species includes the amine in its deprotonated and protonated forms; the third group incorporates the carbamate, also in protonated and deprotonated forms. The protonation constant for the carbamate of MEA is not published and needs to be determined.

Carbamate formation requires the interaction of the deprotonated amine group with the different species of the carbon dioxide/carbonic acid system to form the carbamate. As the reactions are reversible, both protonated and deprotonated forms of the carbamic acid decompose to free amine and carbonate species. Figure 2 is a graphical illustration for the reaction scheme that forms the basis of our analyses. The horizontal axis represents the pH. The lower part of Figure 2 represents the known aqueous chemistry of CO_2, including the formation of the carbonate system and its protonation equilibria, as well as the protonation equilibrium of the amine.

The vertical direction of Figure 2 represents the interaction of the CO_2/H_2O-system with the amine. There are three feasible pathways for the reaction of MEA with different forms of CO_2:

Reversible reaction of carbonic acid with amine

$$H_2CO_3 + RNH_2 \underset{k_{-7}}{\overset{k_7}{\rightleftharpoons}} RNHCO_2H + H_2O \tag{9}$$

Reversible reaction of bicarbonate with amine

$$HCO_3^- + RNH_2 \underset{k_{-8}}{\overset{k_8}{\rightleftharpoons}} RNHCO_2^- + H_2O \tag{10}$$

Reversible reaction of dissolved carbon dioxide with amine

$$CO_2(aq) + RNH_2 \underset{k_{-9}}{\overset{k_9}{\rightleftharpoons}} RNHCOOH \tag{11}$$

Theoretically, there are additional reaction paths. The first is the potential reaction of the amine with the carbonate ion. This reaction is deemed to be very slow as a nucleophilic attack by the amine nitrogen on the doubly charged anion is likely to be negligible. (This will be confirmed later when the rate constants for the interaction of the amine with carbonic acid and the bicarbonate ion are discussed.) A complete set of possible paths would also include the reactions of the protonated amine with all CO_2 species. However, the protonated amine is not a nucleophile and thus is not expected to be reactive. Other possible reactions and products include the formation of the bicarbamate (urea) and mono- and diesters (carbonates) via the reaction of the alcohol group of MEA with carbonic acid. Other

TABLE 1: Published Rate and Equilibrium Constants for the Reactions of CO_2 in Water and Relevant Constants for the Protonation of MEA and the Ionic Product of Water at 30 °C

reaction	kinetics	equilibrium	references
$CO_2(aq) + H_2O \underset{k_{-1}}{\overset{k_1}{\rightleftharpoons}} H_2CO_3$	$k_1 = 4.68 \times 10^{-2}$ s^{-1} [a]	$K_1 = 1.15 \times 10^{-3}$	Soli et al.[43]
	$k_{-1} = 40.65$ s^{-1}	log $K_1 = -2.94$	
$CO_2(aq) + OH^- \underset{k_{-2}}{\overset{k_2}{\rightleftharpoons}} HCO_3^-$	$k_2 = 1.24 \times 10^4$ M^{-1} s^{-1}	$K_2 = 3.21 \times 10^7$ M^{-1}	Pinsent et al.[44]
	$k_{-2} = 3.86 \times 10^{-4}$ s^{-1} [b]	log $K_2 = 7.51$	
$CO_3^{2-} + H^+ \overset{K_3}{\longleftrightarrow} HCO_3^-$		$K_3 = 1.95 \times 10^{10}$ M^{-1}	Harned et al.[45]
		log $K_3 = 10.29$	
$HCO_3^- + H^+ \overset{K_4}{\longleftrightarrow} H_2CO_3$		$K_4 = 2.46 \times 10^3$ M^{-1} [c]	Harned et al.[46]
		log $K_4 = 3.39$	
$MEA + H^+ \overset{K_5}{\longleftrightarrow} MEAH^+$		$K_5 = 2.24 \times 10^9$ M^{-1}	Bates et al.[47]
		log $K_5 = 9.35$	
$OH^- + H^+ \overset{K_6}{\longleftrightarrow} H_2O$		log $K_6 = 13.83$	Maeda et al.[48]

[a] The rate constant for the reaction of CO_2 with H_2O is defined as the pseudo-first-order rate constant. [b] k_{-2} was calculated based on the principle of microscopic reversibility. [c] The protonation is defined as given in the equation; it is common to define this value differently, using the sum over the concentrations of H_2CO_3 and dissolved CO_2 as 'carbonic acid'.

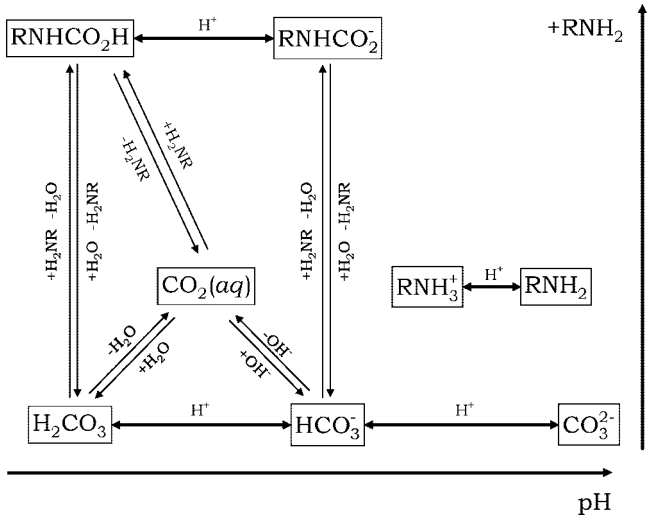

Figure 2. General reaction scheme including all reactions between amine, the CO_2/carbonate group and protons. ↔ represent instantaneous protonation equilibria, ⇄ represent kinetically observable reactions for which rate constants are known or determined in this work.

possible products are the mixed amide-ester (urethane) and a cyclic oxazolidone.[49] None of these has been observed in substantial concentrations in any of the NMR spectra, even at the high concentration used in the present research (minor peaks, ≪1%, do exist but have not been interpreted).

Two major variants of the reaction scheme in Figure 2 were tested against the kinetic and equilibrium measurements. They differ by the paths that lead to the formation of carbamates. Model-variant I consists of the exclusive interaction of the amine with dissolved CO_2(aq), eq 11. This is the mechanism proposed to quantitatively describe the kinetics of CO_2 uptake in wetted-wall experiments.[15,16] In wetted-wall experiments the main source of CO_2 for carbamate formation is directly from the gas phase, and for this type of experiment, the observed kinetics can adequately be described by the exclusive interaction with dissolved CO_2. However, the reaction path for the formation of carbamate via carbonic acid and the carbonate ion cannot be excluded from these experiments. The direct reaction between MEA and CO_2(aq) has also been investigated recently by fast stopped-flow measurements using conductometric data.[30,31] There is also a wealth of older data that has been reviewed.[29] The major CO_2 species present under our NMR experimental conditions is the bicarbonate ion; its known rate of dissociation into aquated CO_2 is significantly slower than the observed formation of the carbamate species. The concentration of CO_2(aq) in our experiment is very low, and its reactivity is negligible with respect to those of the bicarbonate ion and carbonic acid. Thus, this model-variant I results in bad fitting and can be excluded. This apparent contradiction with the published mechanism is the result of the different experimental procedures and observable reactions, rather than mutually exclusive mechanisms.

Model-variant II includes the reactions of CO_2(aq) as well as H_2CO_3 and HCO_3^- with the amine. Figure 3 shows the measured data and fitted curves for two typical NMR measurements. Figure 3A is a kinetic measurement with initial concentration $[MEA]_{tot} = 3.01$ M, $[CO_3^{2-}]_{tot} = 1.20$ M, and $[H^+]_{tot} = 2.83$ M; Figure 3B represents a titration where the concentration ranges are $[MEA]_{tot} = 3.97-2.4$ $[CO_3^{2-}]_{tot} = 3-1.8$ M, and $[H^+]_{tot} = 3.0-3.65$. As is clear from both graphs, the model of model-variant II quantitatively describes all our observations.

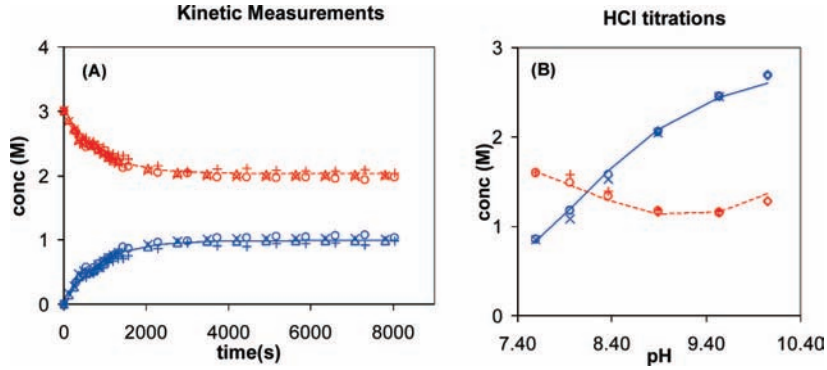

Figure 3. (A) Kinetic concentration profiles measured (markers) and fitted (lines) for the reaction of MEA/HCl with $KHCO_3$; (B) equilibrium concentration profiles measured (markers) and fitted (lines) for the titration of MEA/$KHCO_3$ with HCl. The total amine and carbamate concentrations are indicated in red and blue, respectively.

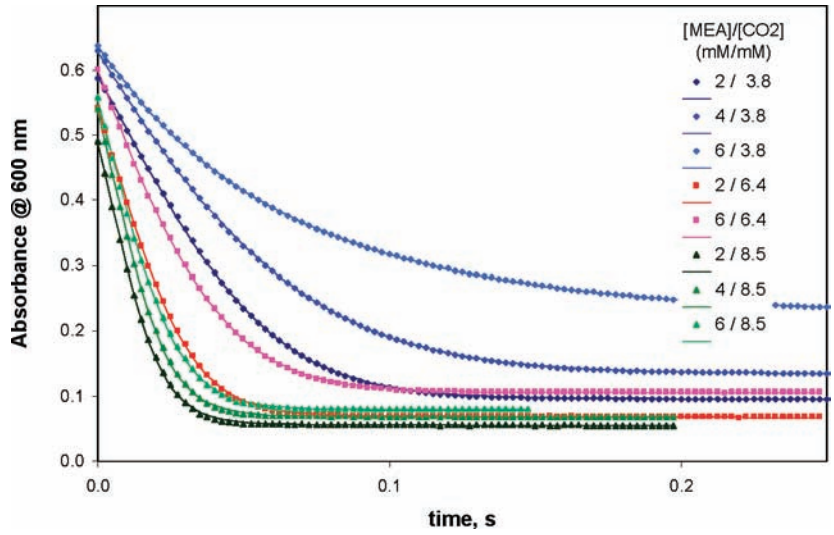

Figure 4. Kinetic traces at 600 nm for measurements with different initial concentrations, as indicated in the legend. Markers represent the measured data, the lines represent the calculated fits.

Figure 3A is a kinetic measurement, the increasing concentrations are the data for the carbamate (blue: markers for experimental; full line for calculated data), and the decreasing (red: markers for experimental; dashed line for calculated data) points represent the free amine. The data markers represent only the resolved peaks: ○ and Δ represent the concentrations for resolved peaks for the amine-methylene (first and repeat measurements), the markers × and + represent the alcohol-methylene group. Figure 3B represents an equilibrium measurement, the addition of HCl solution to a mixture of MEA, HCl, and bicarbonate. The initial main species at high pH is carbamate (blue, full line); below pH 8.4 the major species is the free amine (red, dashed line). Note that there is an overall dilution from high to low pH.

Figure 4 represents measured data and fitted curves for the fast reactions between dissolved CO_2(aq) and MEA, observed at 600 nm. At this wavelength the increase of the protonated form of thymol blue is observed. The measurements are surprising, as the kinetics at higher MEA concentration appears to be slower while increasing CO_2 concentration accelerates the rate, as expected for a second-order reaction. The explanation lies in the fact that the pH is followed, via protonation change of the indicator, and increasing [MEA] results in increased buffer action with concomitant slower change in the free proton concentration. Note that all kinetic measurements were fitted together and the fits are essentially perfect.

Table 2 summarizes the results of the analysis based on model-variant II. Because of the principle of microscopic reversibility, not all of the rate constants in this table can be fitted independently. In the loops (CO_2(aq)−H_2CO_3−$RNHCO_2H$) and (H_2CO_3−$RNHCO_2H$−$RNHCO_2^-$−HCO_3^-) any one of the constants can be defined as a function of the others; refer also to Figure 2. This is indicated in the footnote of Table 2. The numbers in parentheses represent error estimates in terms of the last significant digit of the parameters, as supplied by the fitting algorithm. Theoretically, doubling these values results in 90% confidence limits; in reality the errors are usually underestimated.

In the PCC situation, after mass transfer of the gaseous CO_2 into the amine solution, there are three reaction paths available: CO_2 can react with H_2O, OH^-, or the amine. While the rate constants for the reaction with OH^- (1.24×10^4 M^{-1} s^{-1}) and MEA ($6.11(3) \times 10^3$ M^{-1} s^{-1}) are similar, under relevant conditions most CO_2 will take the amine path to form the carbamate as the free concentration of amine exceeds the [OH^-].

It is also interesting to compare the forward reaction rate constants for the interaction of MEA with carbonic acid, $k_7 = 9.16(1) \times 10^2$ M^{-1} s^{-1}, and the bicarbonate ion, $k_8 = 1.05(2) \times 10^{-3}$ M^{-1} s^{-1}. The ratio is some 6 orders of magnitude. A decrease in the reactivity from neutral carbonic acid to singly charged bicarbonate is expected, and we can predict that the interaction with the doubly charged carbonate ion would be slower by a similar factor, effectively making this path unobservable.

Carbamic acid is a very labile molecule; it has two paths for its decomposition, resulting in CO_2(aq) or in H_2CO_3. The

TABLE 2: Rate and Equilibrium Constants for the Reactions of MEA with Carbonic Acid and Bicarbonate, and Protonation Constant for the Carbamate

reaction	kinetics	equilibrium constants: via kinetics	equilibrium constants: via titrations
$H_2CO_3 + RNH_2 \underset{k_{-7}}{\overset{k_7}{\rightleftharpoons}} RNHCOOH + H_2O$	$k_7 = 9.16(1) \times 10^2\ M^{-1}\ s^{-1}$ $k_{-7} = 5.14(8) \times 10^{-3}\ s^{-1}$	$\log K_7 = 5.25(1)$	$\log K_7 = 5.63(2)$
$HCO_3^- + RNH_2 \underset{k_{-8}}{\overset{k_8}{\rightleftharpoons}} RNHCOO + H_2O$	$k_8 = 1.05(2) \times 10^{-3}\ M^{-1}\ s^{-1}$ $k_{-8} = 7.43(4) \times 10^{-5}\ s^{-1}$[a]	$\log K_8 = 1.15(1)$	$\log K_8 = 1.54(2)$
$CO_2(aq) + RNH_2 \underset{k_{-9}}{\overset{k_9}{\rightleftharpoons}} RNHCOOH$	$k_9 = 6.11(3) \times 10^3\ M^{-1}\ s^{-1}$[a] $k_{-9} = 29.8(3)\ s^{-1}$	$\log K_9 = 2.31(1)$	$\log K_9 = 2.69(2)$
$RNHCOO^- + H^+ \overset{K_{10}}{\rightleftharpoons} RNHCOOH$			$\log K_{10} = 7.49(5)$

[a] k_{-8} is computed as $k_{-8} = (k_8 k_{-7} K_{10})/(k_7 K_4)$; k_{-9} is computed as $k_{-9} = (k_9 k_{-7} k_{-1})/(k_7 k_1)$, based on the principle of microscopic reversibility.

$CO_2(aq)$ path is significantly faster and thus determines the kinetic stability. The carbamate is much more stable with a half-life of about 2.5 h at 30 °C, as defined by k_{-8} in Table 2. The actual stability of a solution is of course strongly pH dependent.

The kinetic analysis results in rate constants for forward and back-reactions for all three paths of carbamate formation. This allows the computation of equilibrium constants which can be compared with the values determined from the equilibrium investigations. While the correspondence is not perfect the values are within roughly 0.4 logarithmic units, and considering the complexity of the analysis this is a good result. In fact, it strongly supports the model used for the analysis.

The equilibrium study also allowed the determination of the protonation constant of the carbamate, eq 7 with a value of log $K_{10} = 7.49(5)$. To our knowledge only one other protonation constant of a carbamate has been reported for the carbamate formed with ammonia; its value is log $K = 6.76$ at 25 °C.[7]

There are several studies that report constants for the equilibrium $HCO_3^- + RNH_2$

$$HCO_3^- + RNH_2 \overset{k_8}{\rightleftharpoons} RNHCOO^-$$

s $RNHCOO^-$: $K_8 = 53.5\ m^{-1}$ (molality^{-1}) at 30 °C;[26] $K_8 = 45.5\ M^{-1}$ at $I = 0.0$ M and 40 °C;[50] $K_8 = 27.8\ M^{-1}$ at $I = 0.59$ M and 20 °C.[51] Considering the width of the temperature range and ionic strength, the equilibrium constants are fairly similar and within the range of our values of 14.1 M^{-1} (kinetic determination) and 34.7 M^{-1} (equilibrium analysis).

Other model-variants were tested. Model-variants that exclude either the reaction of the amine with carbonic acid or bicarbonate are significantly inferior. The sum-of-squares is either more than 1 order of magnitude higher (if the reaction of H_2CO_3 with MEA is excluded) or the fitted rate constant for k_9, the reaction of $CO_2(aq)$, is 3 orders of magnitude too low (if the reaction of HCO_3^- is excluded).

Conclusion

Considering the fundamental importance of carbamate formation between carbonic acid and amines in general and its relevance for CO_2 absorption in particular, it is not surprising that there is a wealth of applied research aimed at a quantitative description. It is, however, surprising how little is known about the molecular mechanism, equilibrium, and in particular rate constants of the carbamate formation reactions.

The results of this investigation allow detailed predictions of the equilibria and the kinetics relevant to postcombustion capture (PCC) of CO_2 by aqueous amine (MEA) solutions in fossil fuel-based power plants. In PCC, CO_2 is absorbed at relatively low temperature by aqueous amine solutions and separated from other gases. The temperature of the solution is subsequently raised, and a certain amount of the absorbed CO_2 is released as a pure gas. The cyclic capacity of amine-based PCC is determined by the difference between the equilibrium constants of the amine−CO_2 interaction at the low and high temperatures used in the absorption plant. The cyclic capacity, together with the rates of the interactions, defines the volumes of amine solution required and thus directly influences the plant size and footprint. Ultimately relevant to PCC is also the energy requirement for the cyclic process. The cyclic capacity of the amine solution is of critical importance, as the heat capacity of the solution and thus energy requirement for cyclic heating and cooling is a major energy component.

Earlier investigations on the absorption of CO_2 by aqueous MEA concentrate on the initial absorption of the gas. Considering the cyclic nature of amine-based PCC and the limited desorption of CO_2 in the stripper, it is important to take into consideration also the carbonate species that are present in the amine solution in the absorber column. Only a complete mechanism can quantitatively describe all relevant aspects of the cyclic process.

Carbamate formation is a significant and apparently an undesirable part of the interaction, as it decreases the cyclic capacity of the amine solution. Deprotonation of the carbamic acid at the pertinent pH results in a free proton which is absorbed by a deprotonated amine. Thus, the CO_2:amine ratio is only 1:2. The exclusive Brønstedt acid−base interaction would result in a much more favorable 1:1 ratio. However, the reaction of dissolved $CO_2(aq)$ with MEA to form the carbamate is relatively fast and thus advantageous. Developing new solvent systems for PCC includes the finding of an ideal compromise between

the energy requirements and reaction rates. Such attempts will be strongly supported by the fundamental investigation of carbamate formation. As such, the analysis described in this work is an important step in understanding, and ultimately improving the performance of amine systems for use as CO_2 capture solvents.

We stress again that the global analysis of measurements acquired under a range of different conditions was a fundamental requirement. All of the reactions occur simultaneously, and none of them can be separated from the others and analyzed independently.

Acknowledgment. Financial support by a CSIRO Flagship grant is acknowledged.

Supporting Information Available: The Supplementary Material contains experimental details, all total concentrations of the components for the titrations and the initial concentrations for the kinetics experiments, together with all concentrations as extracted from the NMR peak intervals. A typical NMR spectrum with interpertation is given. This material is available free of charge via the Internet at http://pubs.acs.org.

References and Notes

(1) Metz, B.; Davidson, O.; de Coninck, H.; Loos, M.; Meyer, L. *IPCC Special Report on Carbon Dioxide Capture and Storage*; Cambridge University Press: New York, 2005.
(2) Gibbons, B. H.; Edsall, J. T. *J. Biol. Chem.* **1963**, *238*, 3502–3507.
(3) Liang, J.-Y.; Lipscomb, W. N. *J. Am. Chem. Soc.* **1986**, *108*, 5051–5058.
(4) Lund, V.; Faurholt, C. *Dan. Tidsskr. Farm.* **1948**, *22*, 109–113.
(5) Olsen, J.; Vejlby, K.; Faurholt, C. *Acta Chem. Scand.* **1952**, *6*, 398–403.
(6) Jensen, M. B. *Acta Chem. Scand.* **1957**, *11*, 499–505.
(7) Christensson, F.; Koefoed, H. C. S.; Petersen, A. C.; Rasmussen, K. *Acta Chem. Scand. A* **1978**, *32*, 15–17.
(8) Caplow, M. *J. Am. Chem. Soc.* **1968**, *90*, 6795–9803.
(9) Arstad, B.; Blom, R.; Swang, O. *J. Phys. Chem.* **2007**, *111*, 1222–1228.
(10) Kumar, P. S.; Hogendoorn, J. A.; Versteeg, G. F.; Feron, P. H. M. *AIChE J.* **2003**, *49*, 203–213.
(11) Li, J.; Henni, A.; Tontiwachwuthikul, P. *Ind. Eng. Chem. Res.* **2007**, *46*, 4426–4434.
(12) Crooks, J. E.; Donnellan, J. P. *J. Chem. Soc., Perkin Trans. 2* **1989**, 331–333.
(13) Tautermann, C. S.; Voegele, A. F.; Loerting, T.; Kohl, I.; Hallbrucker, A.; Mayer, E.; Liedl, K. R. *Chem. Eur. J.* **2002**, *8*, 66–73.
(14) Kumar, P. S.; Hogendoorn, J. A.; Versteeg, G. F.; Feron, P. H. M. *AIChE J.* **2003**, *49*, 203–213.
(15) Cullinane, J. T.; Rochelle, G. *Ind. Eng. Chem. Res.* **2006**, *45*, 2531–2545.
(16) Cullinane, J. T.; Rochelle, G. *Fluid Phase Equilib.* **2005**, *227*, 197–213.
(17) Barth, D.; Tondre, C.; Lappal, G.; Delpuech, J.-J. *J. Phys. Chem.* **1981**, *85*, 3660–3667.
(18) Barth, D.; Tondre, C.; Delpuech, J.-J. *Int. J. Chem. Kinet.* **1983**, *15*, 1147–1160.
(19) Penny, D. E.; Ritter, T. J. *J. Chem. Soc., Faraday Trans. 1* **1983**, *79*, 2103–2109.
(20) da Silva, E. F.; Svendsen, H. F. *Ind. Eng. Chem. Res.* **2004**, *43*, 3413–3418.
(21) da Silva, E. F.; Svendsen, H. F. *Int. J. Greenhouse Gas Control* **2007**, *1*, 151–157.
(22) Park, J.-Y.; Yoon, S. J.; Lee, H. *Environ. Sci. Technol.* **2003**, *37*, 1670–1675.
(23) Jacobsen, J. P.; Krane, J.; Svendsen, H. F. *Ind. Eng. Chem. Res.* **2005**, *44*, 9894–9903.
(24) Boettinger, W. *Fortschr.-Ber. VDI, Reihe 3:* **2006**, *851*, 1–209.
(25) Ermatchkov, V.; Pérez-Salado Kamps, Á.; Maurer, G. *J. Chem. Thermodyn.* **2003**, *35*, 1277–1289.
(26) Boettinger, W.; Maiwald, M.; Hasse, H. *Fluid Phase Equilib.* **2008**, *263*, 131–143.
(27) Falk, M.; Miller, A. G. *Vibr. Spectrosc.* **1992**, *4*, 105–108.
(28) Nam Park, S.; Shik Kim, C.; Hwa Kim, M.; Lee, I.-J.; Kim, K. *J. Chem. Soc., Faraday Trans.* **1998**, *94*, 1421–1425.
(29) Versteeg, G. F.; Van Duck, L. A. J.; Van Swaaij, W. P. M. *Chem. Eng. Commun.* **1996**, *144*, 113–158.
(30) Ali, S. H. *Int. J. Chem. Kinet.* **2005**, *37*, 391–405.
(31) Henni, A.; Li, J.-L.; Tontiwachwuthikul, P. *Ind. Eng. Chem. Res.* **2008**, *47*, 2213–2220.
(32) Linde, D.; *CRC Handbook of Chemistry and Physics*, CRC Press, Boca Raton FL: 2007.
(33) Maeder, M.; Neuhold, Y.-M. *Practical Data Analysis in Chemistry*; Elsevier, 2007.
(34) Maeder, M.; Neuhold, Y.-M.; Puxty, G.; King, P. *Phys. Chem. Chem. Phys.* **2003**, *5*, 2836–2841.
(35) Stumm, W.; Morgan, J. J. *Aquatic Chemistry*, 3rd ed.; John Wiley & Sons, Inc.: New York, 1996.
(36) McCann, N.; Maeder, M.; Attalla, M. *Ind. Eng. Chem. Res.* **2008**, *47*, 2002–2009.
(37) Barner, H. E.; Scheuerman, R. V. *Handbook of Thermochemical Data for Compounds and Aqueous Species*; John Wiley and Sons: New York, 1978.
(38) Stern, K. H.; Amis, E. S. *Chem. Rev.* **1959**, 1–64.
(39) Haubrock, J.; Hogendorn, J. A.; Versteeg, G. F. *Chem. Eng. Sci.* **2007**, *62*, 5753–5769.
(40) Bevington, P. R. *Data Reduction and Error Analysis for the Physical Sciences*; McGraw-Hill: New York, 1969.
(41) Pocker, Y.; Bjorkquist, D. W. *J. Am. Chem. Soc.* **1977**, *99*, 6537–6543.
(42) Martell, A. E.; Smith, R. M.; Motekaitis, R. J. *NIST Standard Reference Database 46 Version 6.0 NIST Critically Selected Stability Constants of Metal Complexes, NIST Standard Reference Data* Gaitersburg, MD 20899.
(43) Soli, A. L.; Byrne, R. H. *Mar. Chem.* **2002**, *78*, 65–73.
(44) Pinsent, B. R. W.; Pearson, L.; Roughton, F. J. W. *Trans. Faraday Soc.* **1956**, *52*, 1512–1520.
(45) Harned, H. S.; Scholes, S. R. *J. Am. Chem. Soc.* **1941**, *63*, 1706–1709.
(46) Harned, H. S.; Davis, J. R. D. *J. Am. Chem. Soc.* **1943**, *65*, 2030–2037.
(47) Bates, R. G.; Pinching, G. D. *J. Res. Natl. Bur. Stand.* **1951**, *46*, 349–352.
(48) Maeda, M.; Hisada, O.; Kinjo, Y.; Ito, K. *Bull. Chem. Soc. Jpn.* **1987**, *60*, 3233–3239.
(49) Boettinger, W.; Maiwald, M.; Hasse, H. *Ind. Eng. Chem. Res.* **2008**, *47*, 7917–7926.
(50) Austgen, D. M. Ph.D. Thesis, University of Texas, 1989.
(51) Chan, H. M.; Danckwerts, P. V. *Chem. Eng. Sci.* **1981**, *36*, 229–230.

JP810564Z